SSRG International Journal of Electrical and Electronics Engineering
ISSN: 2348-8379/ https://doi.org/10.14445/23488379/IJEEE-V12I10P103

Volume 12 Issue 10, 21-33, October 2025


*Original Article*

# Modeling of the Process of Electromagnetic Field Creation by Frequency-Selective Microstrip Arrays in Flat Dual-Reflector Antennas

Oleksandr Fyk[1], Illia Fyk [2], Olena Novykova[3], Honchar roman[4], Oleg Nazarenko[5], Nataliia Smyrynska[6], Kostyantyn Vlasov[7], Mykola Glushchenko[8]

[1,6]*Scientific Research Center of the Armed Forces of Ukraine "State Oceanarium" Naval Institute of the National University "Odesa Maritime Academy", Odesa, Ukraine.*
[2]*National Technical University "Kharkiv Polytechnic Institute", Kharkiv, Ukraine.*
[3,7,8]*Department of Military Communications and Informatization, National Academy of the National Guard of Ukraine, Kharkiv, Ukraine.*
[4] *Research Laboratory of Service and Combat Application of the National Guard of Ukraine Research Center of Service and Combat Activity of the National, Kharkiv, Ukraine.*
[5] *Department of Tactics, National Academy of the National Guard of Ukraine, Kharkiv, Ukraine.*

[1]*Corresponding Author : aifleks@ukr.net*

Received: 03 August 2025 Revised: 05 September 2025 Accepted: 04 October 2025 Published: 30 October 2025

***Abstract*** *- The article presents the results of modeling (the Fish model) of the internal electromagnetic field in a dual-mirror antenna. The results of a numerical study of the radiation pattern of flat frequency-selective doubly periodic printed element arrays within a flat dual-mirror antenna are provided. The modeling results of the electromagnetic field and the radiation pattern of a flat dual-mirror antenna with a frequency-selective microstrip array at a frequency of 2.4 GHz are presented using TICRA-GRASP.*

***Keywords*** *- Hybrid mirror antenna, Microstrip antenna array, Frequency-selective array, Integral equation, Microstrip diffraction array, Dual-mirror antenna, Band-stop filter, Bandpass filter, Spatial scattering matrix.*

## 1. Introduction

One of the most common applications of Frequency-Selective Surfaces (FSS), operating in several frequency bands, is Hybrid Mirror Antennas (HMA). In modern Radio-Technical Systems (RTS), Microstrip Antenna Arrays (MAA) are increasingly being used and manufactured using methods of integrated technology, which allows for a significant reduction in size, weight, and cost of antenna devices. Therefore, significant interest in the development of mathematical models for such arrays has not subsided to the present time.

At present, a multitude of mathematical models have been developed (including programs such as CSC, MW Office, and others), describing MAA with varying degrees of accuracy. However, the issue of analyzing reflective MAA and diffraction gratings made from Microstrip Elements (MSE) of arbitrary structure and conducting material has received little attention so far. Specifically, studying the scattering mechanism of Electromagnetic Waves (EMW) by Microstrip Diffraction Gratings (MDG) is of practical interest in the development of various wave converters of the reflective type, antenna fairings, angular filters that reduce side lobes of aperture antennas, antenna electromagnetic limiters for destructive power, etc..

### *1.1. Analysis of Recent Research and Achievements*

In several studies [1, 2] dedicated to the study of parameters of a Microstrip Antenna Array (MAA), the diffraction problem is addressed, though not as a standalone subject, but rather as a means of determining the antenna characteristics, as it is directly used to determine the antenna characteristics of the MAA with different types of excitation. Moreover, in works dedicated to diffraction gratings, arrays with MSE have not been studied.

For example, in the foundational works on wave diffraction on gratings [3, 4], general patterns of wave scattering and specific characteristics of reflective and semi-transparent gratings, comb-type structures, waveguide structures, strip, and dielectric gratings are described. Despite the great diversity, the studied gratings are one-dimensionally

periodic structures, which do not allow the direct use of the results of numerical-analytical studies presented in these works in the development of Microstrip Diffraction Gratings (MDG). Consequently, there is no solution to the electromagnetic equations for describing the field of a flat multi-element, multi-layer antenna array yet [5].

The purpose of the article: To obtain a system of integral equations - a model of the electromagnetic field, frequency-selective surfaces as part of flat dual-reflector antennas.

### *1.2. Substantive Description of the Electromagnetic Model*

Before formulating the boundary problem, let's consider the main simplifying assumptions that allow us to transition from the real MDG to its mathematical model. Let us consider that the planar MDG has enormous electrical dimensions. In such arrays, the main mass of elements in the central region is in almost identical conditions and do not experience edge influences. More fundamental features of its behavior can be quite accurately described by the behavior of MDG parts that are part of infinite arrays. Therefore, the mathematical model of infinite arrays can successfully serve to analyze MDG with large electrical dimensions.

If necessary, the edge wave method can be used [6] to account for finite array sizes. Problem Statement. Let an infinite layer of a homogeneous magnetodielectric (substrate) of thickness (region V2) be located above an infinite perfectly conducting plane. Microstrip Elements (MSEs) of arbitrary shape are located on the surface of the layer at the nodes of a doubly periodic infinitely extended array with a rectangular cell shape (Figure 1), where $d_1$ and $d_2$ are the lattice periods along the x and y axes, respectively.

We will consider MSEs to be perfectly conducting. Impedance pins are located in the substrate layer, shunting each MSE at N points. Impedance pins are leading pins loaded with concentrated loads, each of which has a controlled surface impedance. The distribution of the surface impedance of the concentrated loads along the k-th impedance pin is described by the function Zk (z'). When constructing a mathematical model, the function Zk (z') is given.

To determine Zk (z'), one can use the equivalent circuit of a real microwave device or experimental results for the surface impedance of real controlled loads. Excitation sources j $E_{ст}$, j $M_{ст}$ are located in a volume Vj, which occupies a part of the volume V1 (Figure 1). The volume V1 occupies the entire upper half-space z > 0.

For multi-element Reflecting Antenna Arrays (RAA), the case of excitation by re-radiators of the array with a locally plane wave, created by measuring sources at the location of the RAA, is of the greatest interest, when the distance between the region Vj and the array Rj $\to\infty$, using the local periodicity approximation.

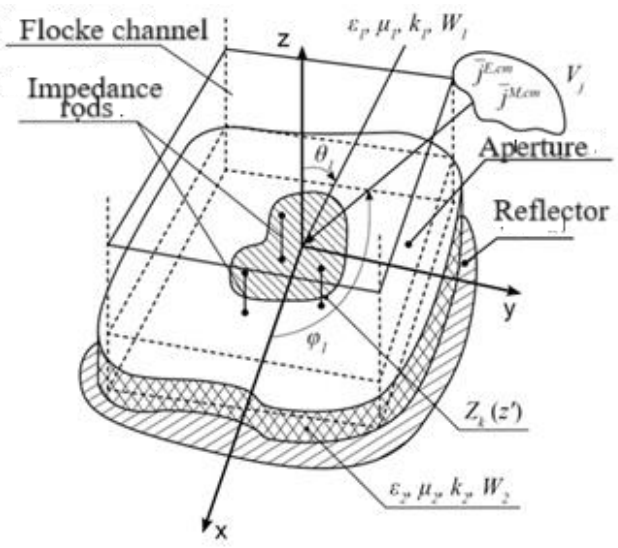


**(a)**

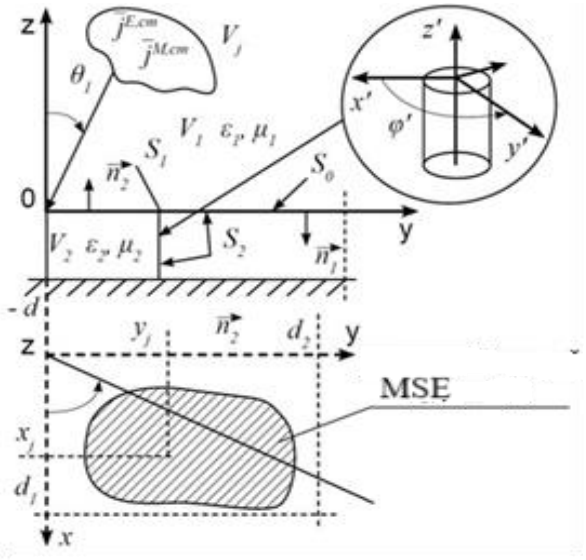


**(b)**

**Fig. 1 Microstrip Reflecting Antenna Array (RAA) with impedance pins: (a) Floquet channel of a reflecting array, and (b) Statement of the electrodynamic problem.**

Parameters of the media in volumes $V_{1,2}$, respectively $\tilde{\varepsilon}_{1,2}$, $\tilde{\mu}_{1,2}$, $k_{1,2}$, $W_{1,2}$. Where $\tilde{\varepsilon}_{1,2}$ $\tilde{\mu}_{1,2}$are, respectively, complex dielectric and magnetic permeability, $k_{1.2}$ is the propagation coefficient, and $W_{1.2}$ is the characteristic resistance. It is necessary to obtain a system of integral equations (IU) describing the task, and to reduce it to a matrix form. The solution of this system will be the desired magnetic current density on the MSE-free surface of the array and the electric current on the impedance rods.

Since the resonance region is of the greatest interest when analyzing the scattering characteristics of a microstrip open antenna array [7], we will use the method of integral equations

[8] to solve the problem. The solution obtained by this method will be general and applicable not only to the resonance region. In addition, it is required that the parabolic antenna operates in N frequency sub-bands: f1 $_1$ f2,..., $f_K$, they use such a technique as spatial separation of parabolic foci and installation of radiators in them, each of which ensures the operation of the mirror antenna (MDA) in one of the K frequency sub-bands.

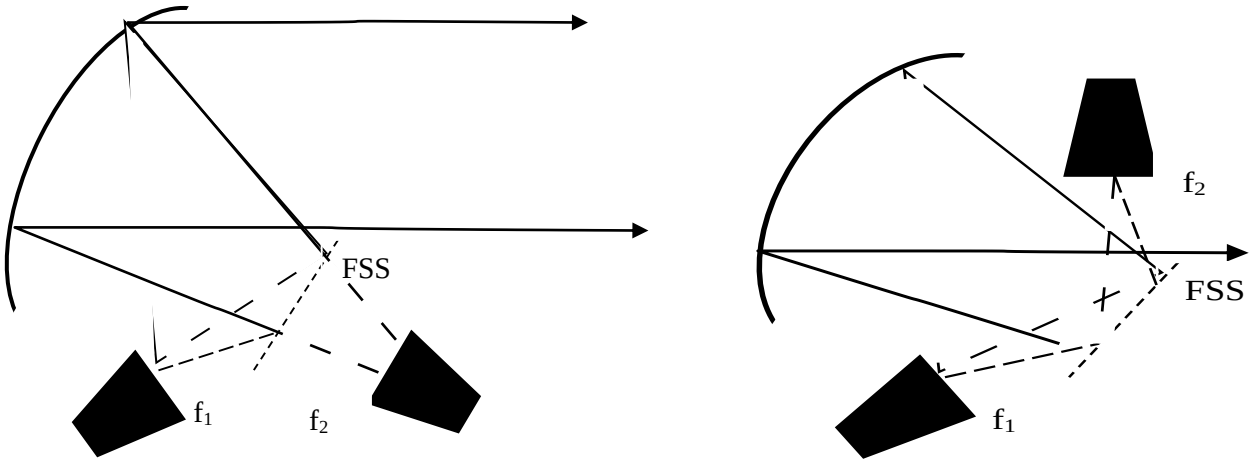


**(a)** **(b)**

**Fig. 2 Multiband radiating FSS with separated radiators (variants a, b)**

We will solve the problem of separating the foci of the parabolic antenna by introducing Frequency-Selective Surfaces (FSS) into its composition. For the case of K=2, the Main Mirror Antenna (MMA) construction scheme looks like the one shown in Figure 2. Frequency-Selective Surface (FSS) in this simple case should have the properties of a Band-Stop Filter (BSF) for Electromagnetic Waves (EMW) of the first sub-band (f1) and a Band-Pass Filter (BPF) for EMW of the second sub-band (f2) in the form of aperture arrays. For the case of K > 2, the FSS must function as a spatially blocking filter (SBF) or a Spatially Transmitting Filter (STF), not in one, but in several sub-bands of the operating frequency range of the MMA. Thus, the FSS must be multi-frequency.

## 2. Formulation of Integral Equations When Constructing a Mathematical Model of a Reflective Microstrip Antenna Array

### *2.1. Integral Relations and Boundary Conditions for a Microstrip Array with Impedance Pins (The Main Antenna Mirror)*

We write the relation for the fields in each of the regions using the Lorentz theorem in integral form. For region V 1 [9]:

$$\int_{\Sigma_1} \{[E_1, H_1^B] - [E_1^B, H_1]\} n_1 \, d\, S' = \\ = \int_{V_1} (j_{B1}^M H_1 - j_{B1}^E E_1) dV' + \\ + \int_{V_1} (j^{E,cm} E_1^B - j^{M,cm} H_1^B) \qquad (1)$$

For region V $_2$

$$\int_{\Sigma_2} \{[E_2, H_2^B] - [E_2^B, H_2]\} n_2 \, d\, S' = \\ = \int_{V_2} (j_{B2}^M H_2 - j_{B2}^E E_2) dV' \qquad (2)$$

Where E $_{1,2}$, H $_{1,2}$, – stress vectors of the sought-after electric and magnetic fields in regions $V_1$ and $V_2$, respectively ; $E_{1,2}^B$ и $H_{1,2}^B$— vectors of the electric and magnetic field strengths of auxiliary sources in $_{V1}$ and $_{V2}$ ; $j_{B_1,B_2}^E$ and $j_{B_1,B_2}^M$ – density of volume currents of auxiliary electric and magnetic sources $V_1$ and $V_2$; $\Sigma_{1)}$ the surface including $S_0$, $S_1$, and the surface of an infinite hemisphere in the region $V_1$ ; $\Sigma_{2)}$ surface containing $S_0$, $S_2$, and $S_k$ – surfaces of all impedance pins; $n_1$ and $n_2$ – external unit normals of the corresponding regions. $A_s$ an auxiliary source for the region $V_2$, we will choose an elementary magnetic vibrator, whose field satisfies the boundary condition:

$$j^{E_{CT}} = j_{(B_1)}^E = 0,\ j_{(B_1)}^M = (I_0^{MB} L)(q - p),\ j^{(M\,cm)} = \\ = (I_0^M L)(q^0 - p) \qquad (3)$$

Where $I_0^M L$– moment of the magnetic current of the excitation source (let us assume that $I_0^M L = 1$, В м), $I_0^{MB} L$, В м – moment of magnetic current of the auxiliary source (we assume that $I_0^{MB} L = 1$, В м) ξ– unit vector defining the orientation of an external source, ν=i $_\tau$or i $_\nu$.

Let the auxiliary source field satisfy the boundary condition E:

$$[n_1, E_1^e]|_{\Sigma_1} = 0. \quad (4)$$

As an auxiliary source for region V2, we will choose an elementary magnetic vibrator, the field of which satisfies the boundary condition:

$$[n_2, E_2^e]|_{\Sigma_2 - S_k} = 0, \quad (5)$$

Where, $S_k$ – Side surfaces of all impedance rods.

On the surface S i, impedance boundary conditions are satisfied [9]:

$$[E_2, n_2]_i = Z_i\left[n_2, [n_2, H_2]\right]_i, \quad (6)$$

Where I means that the quantities included in (6) refer to the i-th impedance pin.

All subsequent expositions are conducted taking into account that the tangential components of the electric field intensity vector on ideally conducting boundaries are equal to zero, as well as taking into account the radiation conditions at infinity.

### *2.2. Integral Equation for a Microstrip Array without Impedance Stubs*

Since, firstly, the electrodynamic analysis of microstrip ARAs, not only containing impedance stubs, but without them (for example, an auxiliary mirror), is of considerable practical interest and, secondly, for the convenience of presenting the procedure for constructing a mathematical model of a microstrip-pin phased array antenna, it is first necessary to formulate a system of Integral Equations (IE). Expression (1), taking into account (4) and (3), will take the form:

$$\int_{S_0}[E_1, H_1^B]n_1 dS = vH_1(p) - H_1^B(q^0, p), \quad (7)$$

Where $S_0$ – surface of the array, free from microstrip elements.

Expanding the vector product in the Cartesian coordinate system (5), we obtain an expression for the magnetic field strength vector in the region $V_1$.

$$\int_{S_0} E_{(1_y)}(q)H^B_{(1_x)}(q,p) - E_{(1_x)}(q)H^B_{(1_y)}(q,p)dS_q + \\ +\xi H_1^B(q^0,p) = vH_1(p) \quad (8)$$

Thus, an expression for the magnetic field intensity in the region $V_1$ has been obtained. Now, we will obtain an expression for the vector of magnetic field intensity in the region $V_2$. Expression (2), taking into account (5), will take the form:

$$vH_2(p) = \int_{S_0}[E_2, H_2^B]n_2 dS'$$

By expanding the vector product in the Cartesian coordinate system, we obtain:

$$vH_2(p) = -\int_{S_0}\left\{E_{(2_y)}, H^B_{(2_x)} - E_{(2_x)}, H^B_{(2_y)}\right\}dS'. \quad (9)$$

Expression (9) will be rewritten as:

$$-\int_{S_0}\begin{Bmatrix} E_{(2_y)}, H^B_{(2_x)}(q,p) - \\ -E_{(2_x)}(q), H^B_{(2_y)}(q,p)\end{Bmatrix}dS_q = \\ = vH_2(p) \quad (10)$$

Consequently, the expression for the magnetic field intensity vector in the region V 2 has been obtained. Omitting the observation point g on the boundary $S_0$ (Figure 1, Figure 3) and maintaining the continuity conditions of the contacting field components, on the boundary of the division, including. $E_{1x}|_{S_0} = E_{2x}|_{S_0} = E_x|_{S_0},\ E_{1y}\big|_{S_0} = E_{2y}\big|_{S_0} = E_y\big|_{S_0},$ $H_{1x}|_{S_0} = H_{2x}|_{S_0} = H_x|_{S_0},\ H_{1y}\big|_{S_0} = H_{2y}\big|_{S_0} = H_y\big|_{S_0},$ From (8) and (10), we obtain a system of two integral equations with respect to the tangential components of the electric field strength vector $E_x(q)$ and $E_y(q)$ on $S_0$. In order to meet the conditions,

$$H_{1x}|_{S_0} = H_{2x}|_{S_0},\ H_{1y}\big|_{S_0} = H_{2y}\big|_{S_0}, \quad (11)$$

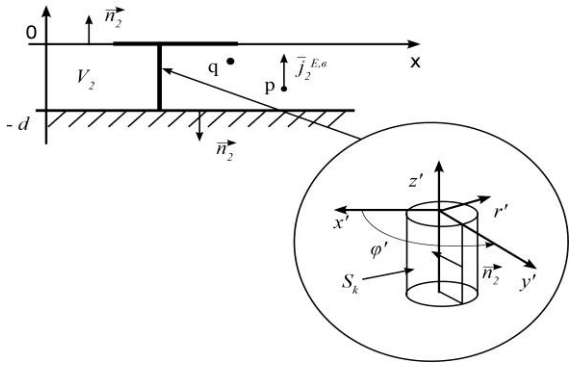


**Fig. 3 Separate cylindrical coordinate system on an impedance rod**

Write the ratio for the components Hx and Hy separately. To obtain an expression for the magnetic field strength vector H x component, it is necessary, as an auxiliary source, to select an elementary magnetic vibrator with a single moment $v=1_x$. Submit v in (8) and (10), get for regions $V_1$ and $V_2$, respectively:

$$vH_{1x}(p) = \int_{S_0} \{E_{(1y)}(q)\widetilde{H}^B_{(1x)}(q,p) - E_{(1x)}(q)\widetilde{H}^B_{(1y)}(q,p)dS_q + \xi H^B_1(q^0,p) \quad (12)$$

$$H_{2x}(p) = -\int_{S_0} \begin{Bmatrix} E_{(2y)}, \widetilde{H}^B_{(2x)}(q,p) - \\ E_{(2x)}(q), \widetilde{H}^B_{(2y)}(q,p) \end{Bmatrix} dS_q \quad (13)$$

Satisfying condition (11) for the x-components of the magnetic field strength vector, from (12) and (13), we obtain the first integral equation of the system:

$$\int_{S_0}^{\int} \begin{Bmatrix} E\,q)\left[\widetilde{H}^B_{(1x)}(q,p) + \widetilde{H}^B_{2x}(q,p\right]_y \\ E_x(q)\left[\widetilde{H}^B_{(1y)}(q,p) + \widetilde{H}^B_{2y}(q,p\right]_q \end{Bmatrix} = -\xi\widetilde{H}^B_1(q^0,p) \quad (14)$$

Where $\widetilde{H}^{\text{в}}_{1x}$, $\widetilde{H}^{\text{в}}_{2x}$, $\widetilde{H}^{\text{в}}_{1y}$, $\widetilde{H}^{\text{в}}_{2y}$–Tangential components of the magnetic field intensity vectors of auxiliary sources are created in each of the regions by an elementary magnetic vibrator with a unit moment oriented along the x-axis. To obtain the relationship defining the magnetic field intensity vector Hy component, it is necessary to choose an elementary magnetic vibrator with a unit moment v = l $_y$ as an auxiliary source. After substituting v in (8) and (10) and satisfying condition (11) for the y-components of the magnetic field intensity vector, we obtain the second IE of the system:

$$\int_{S_0}^{\int} \begin{Bmatrix} E\,q)\left[\widehat{H}^B_{(1x)}(q,p) + \widehat{H}^B_{2x}(q,p\right]_y \\ E_x(q)\left[\widehat{H}^B_{(1y)}(q,p) + \widehat{H}^B_{2y}(q,p\right]_q \end{Bmatrix} = -\xi\widehat{H}^B_1(q^0,p) \quad (15)$$

Where $\widehat{H}^{\text{в}}_{1x}$, $\widehat{H}^{\text{в}}_{2x}$, $\widehat{H}^{\text{в}}_{1y}$, $\widehat{H}^{\text{в}}_{2y}$– components of the stress vector of auxiliary fields formed in each of the regions by an elementary magnetic vibrator with a unit moment oriented along the y-axis.

## 3. Using the Periodicity Condition of Printed Elements in Gratings

Since periodic MSE gratings are considered, S 0 in the periodically repeating Equations (14) and (15) is the system of apertures SA. By the aperture SA, we mean the part of the surface of the unit cell of the grating not occupied by the MSEs located on it. Taking this into account, (14) and (15) will take the form:

$$\sum_{M=-\infty}^{\infty}\sum_{N=-\infty}^{\infty}\int_{S_A} \begin{Bmatrix} E_y(x' + Md_1, y' + Nd_2) \times \\ \times\left[\widetilde{H}^e_{1x}(x' + Md_1, y' + Nd_2; x, y)\right] - \\ +\widetilde{H}^e_{2x}(x' + Md_1, y' + Nd_2; x, y)) \\ -E_x(x' + Md_1, y' + Nd_2) \times \\ \times\left[\widetilde{H}^e_{1y}(x' + Md_1, y' + Nd_2; x, y) + \right] \\ \widetilde{H}^e_{1y}(x' + Md_1, y' + Nd_2; x, y) \end{Bmatrix} dx'dy' = -\xi\widetilde{H}^e_1(q^0,p), \quad (16)$$

$$\sum_{M=-\infty}^{\infty}\sum_{N=-\infty}^{\infty}\int_{S_A} \begin{Bmatrix} E_y(x' + Md_1, y' + Nd_2) \times \\ \times\left[\hat{H}^e_{1x}(x' + Md_1, y' + Nd_2; x, y)\right] - \\ +\hat{H}^e_{2x}(x' + Md_1, y' + Nd_2; x, y)) \\ -E_x(x' + Md_1, y' + Nd_2) \times \\ \times\left[\hat{H}^e_{1y}(x' + Md_1, y' + Nd_2; x, y) + \right] \\ \hat{H}^e_{1y}(x' + Md_1, y' + Nd_2; x, y) \end{Bmatrix} dx'dy' = -\xi\hat{H}^e_1(q^0,p), \quad (17)$$

Where d $_1$ and d $_2$ are the periods of the array along the x and v axes, respectively, M and N are the indices of element-by-element summation.

### *3.1. Definition of the Right-Hand Sides of Integral Equations (16) and (17)*

For the determination of the right side of (16), it is necessary to find the components $\widetilde{H}^{\text{B}}_{1X}(q^0,p)$ и $\widetilde{H}^{\text{B}}_{1Y}(q^0,p)$. For the determination of the right side of (17), it is necessary to find the components $\hat{H}^{\text{B}}_{1X}(q^0,p)$ и $\hat{H}^{B}_{1Y}(q^0,p)$. Then the components of interest to us are [9]:

$$\left.\begin{aligned} H^{e}_{1,2x} &= \frac{1}{i\omega\mu_{1,2}}\left(k^2_{1,2} + \frac{\partial^2}{\partial x^2}\right)A^{\text{мв}}_{1,2x} \\ H^{e}_{1,2y} &= \frac{1}{i\omega\mu_{1,2}}\frac{\partial^2 A^{\text{мв}}_{1,2x}}{\partial x\partial y} \end{aligned}\right\} \quad (18)$$

$$\left.\begin{aligned} H^{e}_{1,2x} &= \frac{1}{i\omega\mu_{1,2}}\left(k^2_{1,2} + \frac{\partial^2}{\partial y^2}\right)A^{\text{мв}}_{1,2y} \\ H^{e}_{1,2y} &= \frac{1}{i\omega\mu_{1,2}}\frac{\partial^2 A^{\text{мв}}_{1,2y}}{\partial x\partial y} \end{aligned}\right\} \quad (19)$$

Where,

$$A^{MB}_{1\{y\}^x} = \frac{1}{4\pi}\left(\frac{exp(-ik_1R_1)}{R_1} + \frac{exp(-ik_1R_2)}{R_2}\right) \quad (20)$$

Where $R_1 = \sqrt{(x-x')^2 + (y-y')^2 + (z-z')^2}$,

$$R_2 = \sqrt{(x-x')^2 + (y-y')^2 + (z+z')^2}$$

Performing the necessary calculations for this case, we obtain from (18) and (19) the following relationships:

$$\widetilde{H}^B_{1X} = \frac{2iG}{k_1W_1}\left[\frac{D}{R_{q^0p}} - EA^2 - k_1^2\right], \quad (21)$$

$$\widetilde{H}^B_{1Y} = \frac{2iG}{k_1W_1}ABE, \quad (22)$$

$$\hat{H}^B_{1X} = \frac{2iG}{k_1W_1}ABE, \quad (23)$$

$$\hat{H}_{1Y}^{B} = \frac{2iG}{k_1 W_1}\left[\frac{D}{R_{q^0p}} - EB^2 - k_1^2\right], \quad (24)$$

$$A = \frac{x^0 - x}{R_{q^0p}}, \quad B = \frac{y^0 - y}{R_{q^0p}}, \quad D = \frac{1 + ik_1 R_{q^0p}}{R_{q^0p}},$$
$$E = D^2 + \frac{D}{R_{q^0p}} + \frac{1}{R_{q^0p}^2}, \quad G = \frac{1}{4\pi}\frac{exp(-ik_1 R_{q^0p})}{R_{q^0p}},$$
$$R_{q^0p} = \sqrt{(x^0 - x)^2 + (y^0 - y)^2 + z^{02}}.$$

Let the external source be located in a distant zone$R_{q^0p}$, i.e., connect the origin with some point p, which is located on the surface $S_0$ (Figure 3). The expression for the distance$R_{q^0p}$ between the point p, belonging to the surface $S_0$, and the point q0, where the external source is located, can be simplified (Figure 4):

$$R_{q^0p} = R - sin\,\theta_i\,(x\,cos\,\varphi_1 + y\,sin\,\varphi_1).$$

Then expressions (21)–(24) will look,

$$\tilde{H}_{1x}^{B}(q^0, p) = \frac{2iG^0}{W_1} k_1[(sin\,\theta_i\,cos\,\varphi_i)^2 - 1], \quad (25)$$

$$\tilde{H}_{1y}^{B}(q^0, p) = \frac{2iG^0}{W_1} k_1\,sin^2\,\theta_i\,cos\,\varphi_i\,sin\,\varphi_i, \quad (26)$$

$$\hat{H}_{1x}^{B}(q^0, p) = \frac{2iG^0}{W_1} k_1\,sin^2\,\theta_i\,cos\,\varphi_i\,sin\,\varphi_i, \quad (27)$$

$$\hat{H}_{1y}^{B}(q^0, p) = \frac{2iG^0}{W_1} k_1[(sin\,\theta_i\,sin\,\varphi_i)^2 - 1], \quad (28)$$

Where, $G^0 = \frac{e^{-ik_1 R}}{4\pi\,R} e^{ik_1\,sin\,\theta_i(x\,cos\,\varphi_i + y\,sin\,\varphi_i)}$.

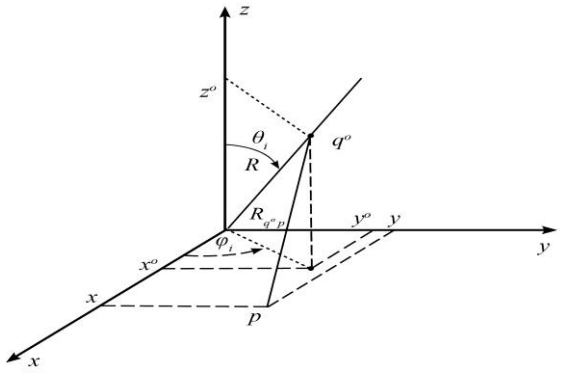


**Fig. 4 Determination of the right-hand sides of the system of integral equations**

Now, to determine the right-hand sides in the integral Equations (14) and (15), which are scalar products, $-\xi \cdot \hat{H}_1^B(q^0, p)$ it is necessary to find the vector. We will require such an orientation of the vector □- that, in the case of perpendicular polarization, the projection of the vector $H(p, t_0)$ -, and in the case of parallel polarization, the projection of the incident wave vector can be represented as:

$$\begin{Bmatrix} H(p, t_0) \\ E(p, t_0) \end{Bmatrix} = (1_x \cdot cos\,\varphi_i + 1_y \cdot sin\,\varphi_i) \cdot H_0 \cdot \begin{Bmatrix} 1 \\ W_1 \end{Bmatrix},$$

Where $H_0 = \frac{k_1\,sin\,\theta_i}{4\pi \cdot R_{qp} W_1}$. $H(p, t_0)$ $E(p, t_0)$– Instantaneous values of magnetic and electric field strength vectors at zero.

However, for the case of perpendicular and parallel polarizations, the projection of the vector ξ onto the plane XOY should look like this:

$$\xi_{XOY}^{\perp} = -1_x \cdot cos\,\varphi_i - 1_y \cdot sin\,\varphi_i,$$

$$\xi_{XOY}^{||} = -1_x \cdot sin\,\varphi_i + 1_y \cdot cos\,\varphi_i. \quad (29)$$

By setting the vector □ in this way, we obtain the following expressions for the right-hand sides of Equations (14) and (15).

$$-\xi \cdot \tilde{H}_1^B(q^0, p) = \\ = -2H_0\,cos\,\varphi_i\,cos\,\theta_1\,e^{ik_1\,sin\,\theta_i(x\,cos\,\varphi_i + y\,sin\,\varphi_i)}, \quad (30)$$

$$-\xi \cdot \hat{H}_1^B(q^0, p) = \\ = -2H_0\,sin\,\varphi_i\,cos\,\theta_1\,e^{ik_1\,sin\,\theta_i(x\,cos\,\varphi_i + y\,sin\,\varphi_i)}. \quad (31)$$

Case of parallel polarization:

$$-\xi \cdot \tilde{H}_1^B(q^0, p) = \\ = -2H_0\,sin\,\varphi_i\,e^{ik_1\,sin\,\theta_i(x\,cos\,\varphi_i + y\,sin\,\varphi_i)}, \quad (32)$$

$$-\xi \cdot \hat{H}_1^B(q^0, p) = \\ = 2H_0\,cos\,\varphi_i\,e^{ik_1\,sin\,\theta_i(x\,cos\,\varphi_i + y\,sin\,\varphi_i)}. \quad (33)$$

Thus, expressions for the right-hand sides of the system of scalar integral Equations (14), and (15) are obtained, corresponding to the cases of excitation of the microstrip array by a locally plane wave of perpendicular and parallel polarization.

Since the array is excited by a locally plane wave, then, as follows from the expressions (30)-(33), the array elements are excited with equal amplitude, and the phase change of the excitation field from element to element is described by a linear law. Considering in (30), (31):

x=Md$_1$, y=Nd$_2$ we get that the lattice cell with number M, N is excited by the field $F \cdot exp[i(h_1 M d_1 + h_2 N d_2]$, Where F – complex amplitude of the excitation field on the cell with number (0,0); $h_1 = k_1\,sin\,\theta_i\,cos\,\varphi_i$, $h_2 = k_1\,sin\,\theta_i\,sin\,\varphi_i$; $k_1 = \omega\sqrt{\varepsilon_1 \mu_1}$– coefficient of wave propagation in the volume;

$\theta_i$–angle of incidence of the exciting locally plane wave, measured from the z-axis; $\varphi_i$ –angle between the plane of incidence and the x-axis is measured in the XOY plane (Figure 1). The components of the electric field intensity vector, which are sought in one transverse section, differ from the components of the electric field intensity vector in another transverse section at a distance that is a multiple of the structure period only by the complex constant:

$$E_{x,y}(x' + Md_1, y' + Nd_2) = \\ = E_{x,y}(x', y') \cdot exp[i(h_1 M d_1 + h_2 N d_2], \quad (34)$$

Where $E_{x,y}(x', y')$– components of the tangential component of the electric field strength vector in the central cell.

This fact is known in the literature as the Floquet theorem [10-13], which is essentially an application of Fourier series theory for periodic functions. It allows for the harmonic expansion of any function whose values are periodically repeated with an accuracy of up to an exponential multiplier.

Such a function describes the magnetic field strengths created on infinite periodic lattices. By using the Floquet theorem, it is possible to find a periodic solution to the Helmholtz equation that satisfies periodic boundary conditions. If we substitute expression (34) into (16) and (17), we get:

$$\int_{S_A} \begin{Bmatrix} E_y(x', y') \cdot K_{11}(x' - x, y' - y) \\ -E_x(x', y') \cdot K_{12}(x' - x, y' - y) \end{Bmatrix} \cdot dx'dy' = \\ = -\xi \tilde{H}_1^e(q^0, p), \quad (35)$$

$$\int_{S_1} \begin{Bmatrix} E_y(x', y') \cdot K_{21}(x' - x, y' - y) - \\ -E_x(x', y') \cdot K_{22}(x' - x, y' - y) \end{Bmatrix} \cdot dx'dy' = \\ = -\xi \hat{H}_1^e(q^0, p), \quad (36)$$

Where the right parts are determined by relations (30) - (33).

### *3.2. Determination of the Kernel Component of the System of Scalar Equations (35), (36)*

Using the relations obtained in [10], we will present the expressions defining the components of the kernel of the system of scalar Equations (35) - (36):

$$K_{11}(x' - x, y' - y) = \\ = \begin{Bmatrix} \left(k_1^2 + \frac{\partial^2}{(\partial x')^2}\right) \frac{G_1^{AR}(x'-x, y'-y)}{i\, k_1 W_1} + \\ + \left(k_2^2 + \frac{\partial^2}{(\partial x')^2}\right) \frac{G_2^{AR}(x'-x, y'-y)}{i\, k_2 W_2} \end{Bmatrix}, \quad (37)$$

$$K_{12}(x' - x, y' - y) = 0$$

$$= \begin{Bmatrix} \frac{\partial^2}{\partial x' \partial y'} \frac{G_1^{AR}(x'-x, y'-y)}{i\, k_1 W_1} + \\ + \frac{\partial^2}{\partial x' \partial y'} \frac{G_2^{AR}(x'-x, y'-y)}{i\, k_2 W_2} \end{Bmatrix}, \quad (38)$$

$$K_{21}(x' - x, y' - y) = \\ = \begin{Bmatrix} \frac{\partial^2}{\partial x' \partial y'} \frac{G_1^{AR}(x'-x, y'-y)}{i\, k_1 W_1} + \\ + \frac{\partial^2}{\partial x' \partial y'} \frac{G_2^{AR}(x'-x, y'-y)}{i\, k_2 W_2} \end{Bmatrix}, \quad (39)$$

$$K_{22}(x' - x, y' - y) = \\ = \begin{Bmatrix} \left(k_1^2 + \frac{\partial^2}{(\partial y')^2}\right) \frac{G_1^{AR}(x'-x, y'-y)}{i\, k_1 W_1} + \\ + \left(k_2^2 + \frac{\partial^2}{(\partial y')^2}\right) \frac{G_2^{AR}(x'-x, y'-y)}{i\, k_2 W_2} \end{Bmatrix}, \quad (40)$$

Where,

$$G_1^{AR}(x' - x, y' - y) = \\ = \frac{1}{d_1 d_2} \sum_{m=-\infty}^{\infty} \sum_{n=-\infty}^{\infty} \frac{1}{\gamma_{1mn}} e^{[i\alpha_m(x'-x) + i\alpha_n(y'-y)]}, \quad (41)$$

$$G_2^{AR}(x' - x, y' - y) = \\ = \frac{1}{d_1 d_2} \sum_{m=-\infty}^{\infty} \sum_{n=-\infty}^{\infty} \frac{cth(\gamma_{2mn} d)}{\gamma_{2mn}} e^{[i\alpha_m(x'-x) + i\alpha_n(y'-y)]}, \quad (42)$$

$$\left.\begin{aligned} \alpha_m &= \frac{2\pi\, m}{d_1} + h_1,\ \alpha_n = \frac{2\pi\, n}{d_2} + h_2 \\ \gamma_{1mn} &= \sqrt{\alpha_m^2 + \alpha_n^2 - k_1^2} \\ \gamma_{2mn} &= \sqrt{\alpha_m^2 + \alpha_n^2 - k_2^2} \end{aligned}\right\} \quad (43)$$

Thus, the use of the periodicity condition allowed us to consider a single central aperture instead of a periodic aperture system. The presence of an environment of identical Microstrip Elements (MSE) and its influence on the characteristics of the central lattice element are taken into account by the functions $G_1^{AR}(x' - x, y' - y)$ $G_2^{AR}(x' - x, y' - y)$, which are defined by (41), and (42). From the above relations, the fields of infinite microstrip element lattices can be obtained and represented as double infinite series over the spatial harmonics of the system. The finite number of these harmonics (for lower values of t and p) are propagating in the direction of the z-axis ($\gamma_{1mn}$– imaginary quantity), and an infinite number of harmonics (for sufficiently large t and p) are decaying in this direction ($\gamma_{1mn}$– real quantity).

## 4. Numerical Solution of the System of Integral Equations (SIE)

### *4.1. The Method of Moments for Solving the System of Integral Equations (IE)*

Electrodynamic integral equations rarely have analytical solutions.

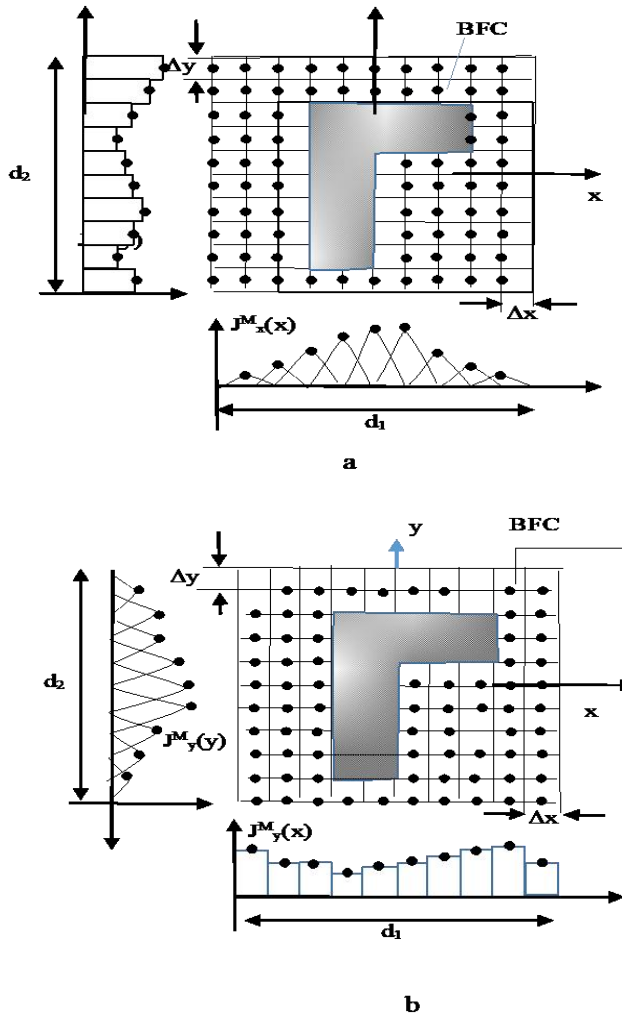


**Fig. 5 Decomposition of the aperture's magnetic current by basis functions**

The number of such solutions is very small, so in most cases, numerical methods must be used to solve the System of Integral Equations (SIE). There are several methods for solving IE, but in electrodynamics, the

most widespread is the method of moments [2, 13], which involves choosing a system of Basic Functions for Currents (BFC) to decompose the unknown function, defining a system of Test Functions (TF), taking the scalar product of each test function with the left and right parts of the IE, resulting in a System of Linear Algebraic Equations (SLAE). By solving this system, the coefficients of the decomposition of the unknown function are determined. The most common special cases of the method of moments are: the Krylov-Bogolyubov method (basis functions – piecewise constant, test functions – delta functions) and the Galerkin method (identical basis and test functions). For the numerical solution of the system IE (44)-(46), the general Galerkin method was used:

$$\int_{S_A}\begin{Bmatrix}J_x^M(x',y')K_{11}(q,p)+\\+J_y^M(x',y')K_{12}(q,p)\end{Bmatrix}dS_q - \\ -i\ 2\pi\ a\sum_{k=1}^{Nk}\int_{-d}^{0}J_{zk}^{э}(z')K_{13}(x_k,y_k,z';p)dz' = \\ = -\xi\widetilde{H}_1^{e}(q^0,p), \quad (44)$$

$$\int_{S_A}\begin{Bmatrix}J_x^M(x',y')K_{21}(q,p)+\\J_y^M(x',y')K_{22}(q,p)\end{Bmatrix}dS_q - \\ -i\ 2\pi\ a\sum_{k=1}^{Nk}\int_{-d}^{0}J_{zk}^{э}(z')K_{23}(x_k,y_k,z';p)\cdot dz' = \\ = -\xi\widehat{H}_1^{e}(q^0,p) \quad (45)$$

$$\int_{S_A}\begin{Bmatrix}J_x^M(q)K_{31}(q;x_t,y_t,z)+\\J_y^M(q)K_{32}(q;x_t,y_t,z)\end{Bmatrix}dS_q - \\ -2\pi\ a\sum_{k=1}^{N}\int_{-d}^{0}J_k^{э}(z')K_{33}(x_k,y_k,z';x_t,y_t,z)dz' = \\ = Z_t(z)J_t^{э}(z) \quad (46)$$

Where $t = 1\ldots N$ $J_x^M(q), J_y^M(q)$– components of the surface density of the magnetic current of the aperture, determined by the relation:

$$J_x^M(q) = E_y(q), J_y^M(q) = -E_x(q) \quad (47)$$

Integral Equations (44), and (45) are component-wise representations of the vector integral equation, representing the boundary condition for the magnetic field in the aperture of the array.

Selection of Pasis and trial functions. One of the main problems in the numerical investigation of the integral equation (ip) is the choice of a system of basis functions that approximates the actual current distribution function. A successful choice of this system of functions leads to faster convergence of the solution and reduces computational volume. The basic functions should reflect the characteristic features of the actual current distribution, in particular, at the edge of the MSE, the normal component of the magnetic current in the aperture should go to zero as the square root of the distance to the edge, and the tangential component should behave as the inverse of the square root.

When choosing basis functions, the ability to calculate integrals in an analytical form and a sufficiently simple form of the resulting expressions is of great importance.

In the case of an arbitrary MSE form, to convert IE into SLAE, one can use the finite element method, borrowing from it the idea of discretizing the domain of the sought current and piecewise polynomial approximation. The simplest path is to use triangular-shaped elements in the discretization and linear

approximation of the sought function within the triangles. However, when the domain of the sought current can be divided into rectangular subdomains, it is convenient to choose two-dimensional functions of subdomains as BFC, as used in [7]. Each of these functions is a product of triangular pulses along the current flow direction and rectangular pulses in the perpendicular direction. As a result, an overlapping distribution of basic functions for the orthogonal current components is obtained (Figure 5). The main feature of the basis shown in Figure 5 is that its application allows obtaining a current representation not only on the MSE of arbitrary shape, but also taking into account the field features at the edges. The application of this basis for the current allows eliminating the non-integrated component of the kernel in the vector IE (35)-(36), which arises when introducing the differential operator under the summation sign in expressions (37)-(40). Using this representation of current, or the decomposition into Basis Functions of Current (BFC) with finite power, and the formal application of the method of moments, allows, by integration by parts, to transfer the differentiation operation from the IE kernel to the current to be found.

So, let us perform the decomposition of the current distribution functions, which are defined as system functions, each of which is the product of a piecewise-triangular function $T_m(t)$ along the direction of current flow and a piecewise-constant function $P_m(t)$ in the perpendicular direction.

$$J_x^M(x',y') = \sum_{i=2}^{Lx}\sum_{j=1}^{Ly} A_{ij}\cdot T_i(x')\cdot P_j(y'), \quad (48)$$

$$J_y^M(x',y') = \sum_{i=2}^{Lx}\sum_{j=1}^{Ly} B_{ij}\cdot T_j(y')\cdot P_i(x'), \quad (49)$$

Where,

$$P_i(t) = \begin{cases} 1, & npu \quad t \in (t_i, t_{i+1}); \\ 0, & npu \quad t \notin (t_i, t_{i+1}), \end{cases} \quad (50)$$

$$T_i(t) = \frac{(t - t_{i-1})}{\triangle t} \; npu \; t \in (t_{i-1}, t_i);$$
$$T_i(t) = \frac{(t_{i+1} - t)}{\triangle t} \; npu \; t \in (t_i, t_{i+1});$$
$$T_i(t) = 0 \; npu \; t \notin (t_{i-1}, t_{i+1}). \quad (51)$$

Here are designated: $A_{ij}$ and $B_{ij}$ – coefficients of magnetic current expansion, which need to be determined, $\Delta t = t_{i+1} - t_i$ – a partition interval of the integration section along the corresponding coordinate.

Note that, by choosing a non-uniform array for aperture partitioning, a variable interval, it is possible to use a small number of basis functions and simultaneously well approximate the magnetic current near the edges of MSEs. To do this, it is necessary to decrease when approaching the edge of MSEs. Thus, it is possible to take into account quite accurately the features of the magnetic current distribution of the aperture near the edges of MSEs. At the same time, the number of equations in SLAE increases slightly.

We will decompose the distribution function of the surface density of the electric current of the k-th impedance pin $J_{zk}^э(z')$ into piecewise triangular functions:

$$J_{zk}^э(z') = \sum_{l=0}^{Lz+1} D_{kl} T_l(z' + d), \quad (52)$$

Where $D_{kl}$– decomposition coefficients of the sought current.

In expression (52), the extreme basis functions with numbers l=0 and $l=L_z + 1$ are piecewise trapezoidal, and within the interval – piecewise linear.

### *4.2. Determination of Scattering Calculation Characteristics*

The secondary field of a periodic structure excited by a plane wave represents an infinite set of plane waves. Among them, only a finite number of waves propagate, and the rest quickly attenuate. In a single-wave mode, only the zero spatial harmonic (m=0, n=0) will propagate.

Practical interest is caused by information about the scattering field in the far zone. Obviously, this field is a set of propagating plane waves.

In a single-wave range, only the zero spatial harmonic remains across the entire set. Since the amplitude of this harmonic strongly depends on the polarization of the incident field, and since an incident wave of one polarization (vertical or horizontal) generally excites reflected waves of both polarizations, it is convenient to represent the field, both incident and reflected, as the sum of two components. One of these components has an electric field whose vector of intensity is perpendicular to the plane of incidence (horizontal polarization).

Let us introduce a linear orthogonal polarization basis ( $i_1, i_2$ ) so that the unit vector and 1 of this basis lies in the plane of incidence, and the unit vector and 2 is perpendicular to it. Projecting this basis onto

$$i_1' = i_x \cos\varphi_i + i_y \sin\varphi_i, \quad i_2' = i_x \sin\varphi_i - i_y \sin\varphi_i, \quad (53)$$

Where $i_1'$ and $i_2'$ – projections of vectors $i_1$ and $i_2$ onto the XOY plane.

Let us define the elements of the polarization scattering matrix (PSM) as the ratio of complex amplitudes of orthogonally polarized components of electric field strength vectors of the zero spatial harmonic of the reflected and incident waves:

$$S_{11}=\left.\frac{E^{S(||)}_{(0,0)}i_1'}{E^{J(||)}_{(0,0)}i_1'}\right|_{z=0};\quad S_{12}=\left.\frac{E^{S(||)}_{(0,0)}i_1'}{E^{J(\perp)}_{(0,0)}i_2'}\right|_{z=0};$$
$$S_{21}=\left.\frac{E^{S(\perp)}_{(0,0)}i_2'}{E^{J(||)}_{(0,0)}i_1'}\right|_{z=0};\quad S_{22}=\left.\frac{E^{S(\perp)}_{(0,0)}i_2'}{E^{J(\perp)}_{(0,0)}i_2'}\right|_{z=0}, \qquad (54)$$

Where the superscripts "i" and "s" refer to the incident and reflected fields, respectively, and the subscripts (||) and "(⊥)" denote parallel and perpendicular polarizations, respectively; the subscript (0,0) means that the zero spatial harmonic of the field is included in the ratio (54).

Thus, the PSM elements $S_{11}$ and $S_{22}$ are introduced as reflection coefficients for the zero spatial harmonic on matched polarizations, and the elements $S_{21}$ and $S_{12}$ as cross-polarization coefficients. Let us express the PSM elements through the aperture magnetic current expansion coefficients. For this, we expand the functions $\overset{o}{J}{}^{M}_{x}(x',y')$ $\overset{o}{J}{}^{M}_{y}(x',y')$ in a double Fourier series:

$$\overset{o}{J}{}^{M}_{\{x\}\{y\}}(x,y)=\sum_{m=-\infty}^{\infty}\sum_{n=-\infty}^{\infty}\overset{o}{J}{}^{M}_{\{x\}\{y\}mn}\,e^{\left[-2\pi\, i\left(\frac{mx}{d_1}+\frac{ny}{d_2}\right)\right]}. \qquad (55)$$

Expression (55) is a condensed form of recording two decompositions at once, both for $\overset{o}{J}{}^{M}_{x}(x',y')$ and for $\overset{o}{J}{}^{M}_{y}(x',y')$. The expression for $\overset{o}{J}{}^{M}_{x\,mn}$ $\overset{o}{J}{}^{M}_{y\,mn}$ the decomposition coefficients can be represented as,

$$\overset{o}{J}{}^{M}_{x\,mn}=\sum_{i=2}^{L_x}\sum_{j=1}^{L_y}A_{ij}R_{x\,mn}e_{mn}(x_i,y_j), \qquad (56)$$

$$\overset{o}{J}{}^{M}_{y\,mn}=\sum_{i=1}^{L_x}\sum_{j=2}^{L_y}A_{ij}R_{y\,mn}e_{mn}(x_i,y_j). \qquad (57)$$

Where the coefficients for unknown complex amplitudes of BFS: $R_{x\,mn}$ and $R_{y\,mn}$, as well as $e_{ij\,mn}=e_{mn}(x_i,y_j)$ are defined in (47)

Since in expressions (54), defining the elements of the PMR, only the zero spatial harmonic is distinguished from the entire spectrum of spatial frequencies of the reflected field, then, leaving in (55) the harmonic m = 0, n = 0, taking into account (53) and the relations defining the surface magnetic currents:

$$J^{M}_{1,2,3y}(q)=E_{1,2,3y}(q),$$
$$J^{M}_{1,2,3y}(q)=-E_{1,2,3x}(q)\quad npu\ q\in S_{0,1,2,3};$$

We get:

$$S_{11}=-1+sin\,\varphi_i\sum_{i=2}^{L_x}\sum_{j=1}^{L_y}A_{ij}R_{x00}-$$
$$-cos\,\varphi_i\sum_{i=2}^{L_x}\sum_{j=1}^{L_y}A_{ij}R_{y00}, \qquad (58)$$

$$S_{12}=\frac{sin\,\varphi_i\sum_{i=2}^{L_x}\sum_{j=1}^{L_y}A_{ij}R_{x00}-cos\,\varphi_i\sum_{i=2}^{L_x}\sum_{j=1}^{L_y}A_{ij}R_{y00}}{sin\,\varphi_iE^i_x-cos\,\varphi_iE^i_y}, \qquad (59)$$

$$S_{21}=-\frac{cos\,\varphi_i\sum_{i=2}^{L_x}\sum_{j=1}^{L_y}A_{ij}R_{x00}-sin\,\varphi_i\sum_{i=2}^{L_x}\sum_{j=1}^{L_y}A_{ij}R_{y00}}{cos\,\varphi_iE^i_x-sin\,\varphi_iE^i_y}, \qquad (60)$$

$$S_{22}=-1-$$
$$-\frac{cos\,\varphi_i\sum_{i=2}^{L_x}\sum_{j=1}^{L_y}A_{ij}R_{x00}-sin\,\varphi_i\sum_{i=2}^{L_x}\sum_{j=1}^{L_y}A_{ij}R_{y00}}{sin\,\varphi_iE^i_x-cos\,\varphi_iE^i_y}. \qquad (61)$$

Substituting the expressions for $E^i_{x,y}$ and $R_{x,y00}$ into relations (58)–(61), we obtain the calculation formulas for the elements of the PMR:

$$S_{11}=-1+\tau\frac{cos\,\varphi_i\sum_{i=2}^{L_x}\sum_{j=1}^{L_y}A_{ij}-sin\,\varphi_i\sum_{i=2}^{L_x}\sum_{j=1}^{L_y}A_{ij}}{cos\,\theta_i};$$

$$S_{12}=-\tau\left(cos\,\varphi_i\sum_{i=2}^{L_x}\sum_{j=1}^{L_y}A_{ij}-sin\,\varphi_i\sum_{i=2}^{L_x}\sum_{j=1}^{L_y}A_{ij}\right);$$

$$S_{21}=\frac{-\tau}{cos\,\theta_i}\left(sin\,\varphi_i\sum_{i=2}^{L_x}\sum_{j=1}^{L_y}A_{ij}+cos\,\varphi_i\sum_{i=2}^{L_x}\sum_{j=1}^{L_y}A_{ij}\right);$$

$$S_{21}=-1-\tau\left(sin\,\varphi_i\sum_{i=2}^{L_x}\sum_{j=1}^{L_y}A_{ij}+cos\,\varphi_i\sum_{i=2}^{L_x}\sum_{j=1}^{L_y}A_{ij}\right), \qquad (62)$$

Where, $\tau=\frac{\Delta x\Delta y}{dxdy}$, $\Delta x$ and $\Delta y$– intervals of aperture division (parts of the surface of the unit cell of the gratings that are free from printed elements) along the x and y axes, respectively. Thus, expressions for the S-matrix ||S|| elements have been obtained due to the expansion coefficients (55) of the surface magnetic current of the aperture.

The assumption of the periodicity of the grating allows, using the considered mathematical model, to analyze both printed gratings with elements of complex shape and multi-layer gratings of printed elements. In this case, the consideration of printed gratings with complex shape elements is of interest. Below, printed antenna gratings of the reflecting type are analyzed, and their elements have the shape of geometric fractals.

### *4.3. Features of Modeling a Phase-Correcting Array (PCA) of the Sub Reflector of a Dual-Reflector Antenna*

Let us consider the construction of PCA with improved characteristics based on the MSE of a complex shape. As noted in the previous subsection, plate-like MSEs with stubs are widely used as printed PCA elements, combining the functions of reflecting phase shifters and re-emitters, in

addition to rectangular ones. The idea of using such elements in the construction of Phase-Correcting Twist Reflectors (FCTR) of the folded AR was first proposed in [14], where the operation of a multifunctional Dual-Reflector Antenna (DRA) with MSEs of complex shape was numerically modeled. It was further developed in the works of foreign authors. Thus, [15] describes a folded microstrip reflecting antenna array operating in radar and communication modes, with square MSEs with stubs acting as printed re-emitting elements. The topologies of such elements are shown in Figure 6. At the same time, MSEs act as DRA irradiators under consideration, based on MPDRA.

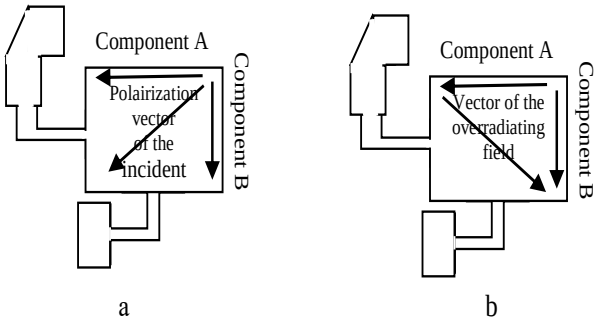


**Fig. 6 Topology of printed circuit elements with phase-correcting twist reflector**

As can be seen from Figure 6(b), each square MSE is rotated relative to the irradiating antenna by an angle of 45°. To realize the effects of polarization plane rotation and focusing upon reflection, two microstrip open stubs, each equipped with a quarter-wave transformer, are attached to each square MSE. Microstrip stubs with transformers are connected to adjacent faces of the square MSE (Figure 6).

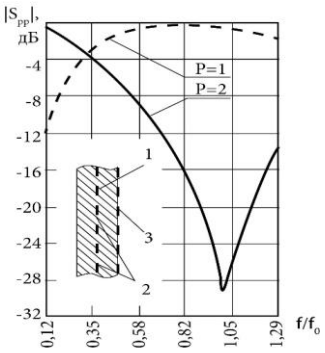


**Fig. 7 Frequency dependencies of the diagonal elements of the SSM grid of slits in the conducting screen, placed on a dielectric substrate, at different angles of incidence of the exciting wave 1–Θ=0°:2–Θ=40°;3–Θ=80°**

The field of the Electromagnetic Wave (EMW), which excites the antenna, is first received by two stubs, then reflected from the open ends of the stubs, and the reflected wave returns to the microstrip re-radiators, which re-radiate it into the surrounding space. The difference in lengths of these open stubs is equal to a quarter of the wavelength.

Such a choice ensures the orthogonality of the polarization vector of the reflected field with respect to the polarization vector of the incident wave. Additionally, the absolute lengths of the stubs are selected according to the location of each square MSE on the canvas of the Reflecting Antenna Array (RAA), to compensate for the phase delay that arises due to the difference in path lengths from the phase center of the irradiator to the MSEs that have different locations on the main planar reflector DRA..

One possible way to overcome the outlined shortcomings is to use a quasi-optical filter as an auxiliary flat reflector of a Cassegrain antenna.

Such a filter can be built on the basis of a multilayer planar array, for example, in the form of perforated slot screens separated by dielectric layers, as shown in Figure 7.

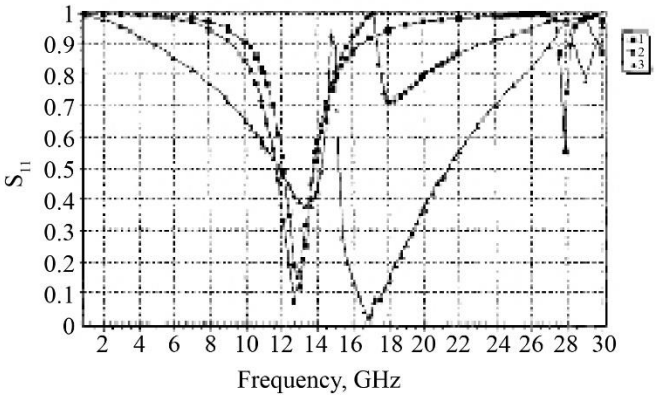


**Fig. 8 Result of the constructive synthesis of the polarization-selective auxiliary conductive reflector of a two-mirror microstrip antenna**

As can be seen from Figure 7, the key element of such a filter is a Frequency-Selective Surface (FSS) of rectangular apertures made in a conductive screen and located on a dielectric substrate of finite thickness. Frequency dependencies of the diagonal elements of the Spatial Scattering Matrix (SSM) of a slit array in a conducting screen placed on a dielectric substrate at various angles of incidence of the exciting wave are shown in Figure 7 [14].

As can be seen from the graphs, if the polarization vector of the incident wave is parallel to the slits, the wave is reflected from this structure. For waves with orthogonal polarization of the Electric Fields (EFs), it acts as a quasi-optical filter, which, on one hand, is a bandpass, permeable Electromagnetic Wave (EMW) filter within a certain frequency range, and on the other hand, it is an angular filter transparent to incident waves within a certain angular sector (Figure 5). Since the auxiliary flat reflector of a Dual-Mirror Antenna (DDA) must be a polarization-selective structure, which in the operating frequency range of the antenna

almost completely reflects the field. Let us consider the possibility of applying such a structure as an auxiliary flat mirror DDA. To minimize energy losses during wave transmission through this structure during its construction, it is necessary to select dielectric layers with low electrical thickness. For numerical analysis of multilayer microstrip reflector antenna arrays (VAR) on thin dielectric substrates, it is advisable to use the algorithm described in [15]. The results of the constructive synthesis of a polarization-selective auxiliary flat mirror DDA are shown in Figure 8. At the cross-section of Figure 8, it is visible that this mirror is a four-layer structure consisting of printed arrays that perform the function of a polarization filter (marked with the number 1), two dielectric layers (marked with the number 2), and a "translucent array" (marked with the number 3).

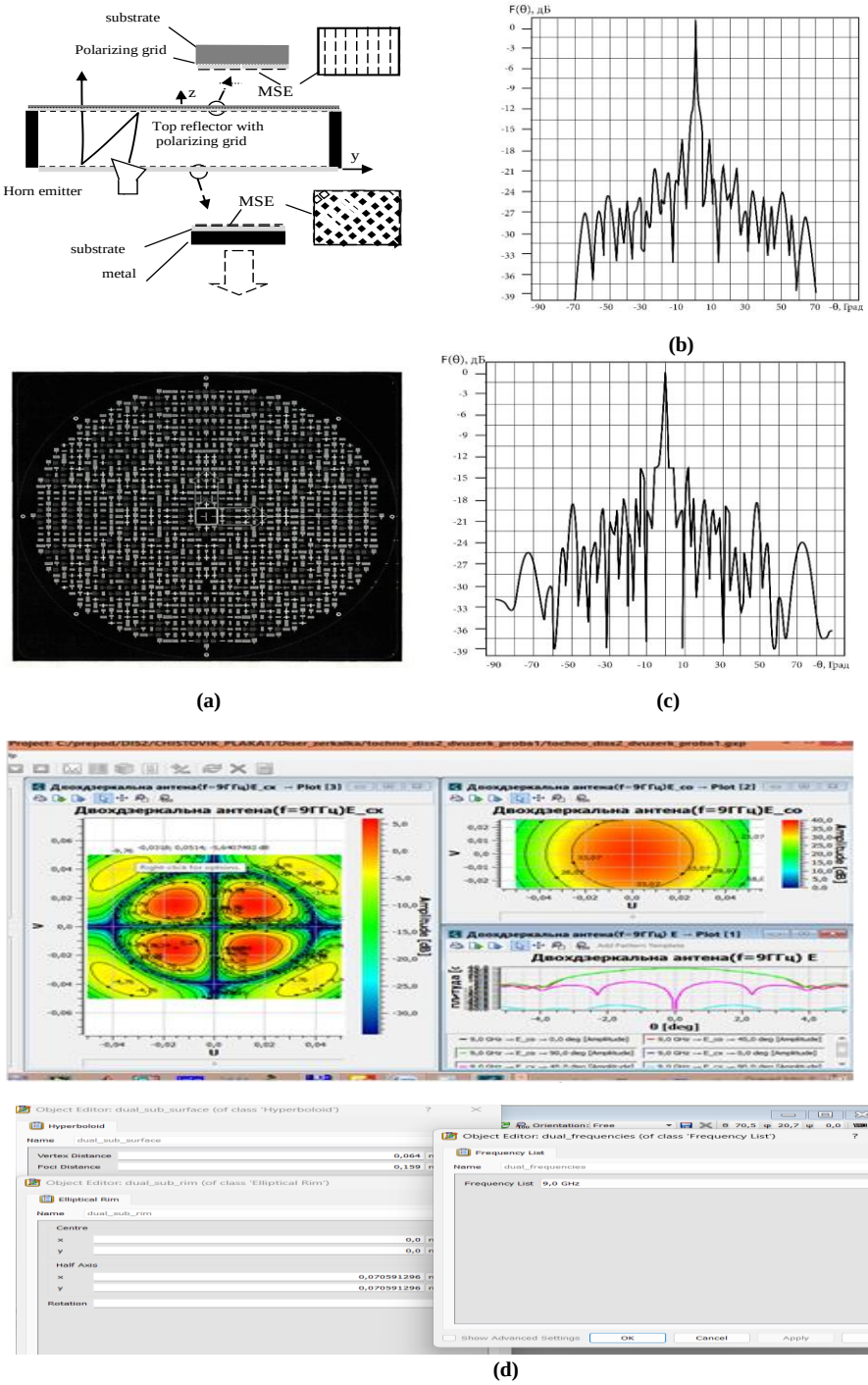


**Fig. 9 Structure of a two-mirror antenna and its directional diagram based on a microstrip reflecting antenna array of printed elements with "internal" feeding: (a) Structure of a flat two-mirror, (b) xOz plane, (c) yOz plan, (d) EMW(TICRA-GRASP).**

## 5. Conclusions

The structure of the two-mirror antenna and the results of modeling its radiation pattern in the program, as well as the currents i, and the radiation pattern of the microstrip element array are presented in Figure 9. The results confirmed the reliability of the mathematical description of the electromagnetic model, which is discussed in the article. As a result of electromagnetic modeling, a two-mirror antenna is proposed that has the following features:

- a significant increase in the antenna array's efficiency (efficiency) - 60%;
- the small area occupied by the radiators makes it possible to reduce:
- the small area occupied by the radiators allows for a reduction in the radar cross-section of such a phased array antenna (PAA) (one microstrip element (MSE) - a vibrator occupies an area of 6x6 mm2 at a frequency of F=2.46 GHz);
- the weak angular sensitivity of the frequency characteristic of the MSE radiators allows for undistorted spatial scanning with the array beam;
- in the presence of a dielectric layer, the mutual influence of the array vibrators is reduced.
- Thus, the proposed dual-reflector antenna can be used to form precise electromagnetic strike systems.

## References


[1] Charles Macon, Keith D. Trott, and Leo C. Kempel, "A Practical Approach to Modeling Doubly Curved Conformal Microstrip Antennas," *Progress in Electromagnetics Research (PIER)*, vol. 40, pp. 295-314, 2003. [CrossRef] [Google Scholar] [Publisher Link]

[2] Chung-Cytz Liu et al., "Plane Wave Reflection from Microstrip-Patch Arrays-Theory and Experiment," *IEEE Transactions on Antennas and Propagation*, vol. 33, no. 4, pp. 426-435, 1985. [CrossRef] [Google Scholar] [Publisher Link]

[3] Robert J. Mailloux, Phased Array Antenna Handbook, 3rd ed., Artech House, 2017. [Google Scholar] [Publisher Link]

[4] Alexander Nikolaevich Sysoev, Mathematical Model of Transmitting KPHAR, *Antennas*, no. 11, pp. 28-29, 2010. [Google Scholar] [Publisher Link]

[5] Simeon M. Metev, and Vadim P. Veiko, *Laser Assisted Microtechnology*, 2nd ed., Springer Berlin, Heidelberg, 1998. [CrossRef] [Google Scholar] [Publisher Link]

[6] Xin-Kuan Wang, and Gui-Bao Wang, "A Hybrid Method Based on the Iterative Fourier Transform and the Differential Evolution for Pattern Synthesis of Sparse Linear Arrays," *International Journal of Antennas and Propagation*, vol. 2018. pp. 1-7, 2018. [CrossRef] [Google Scholar] [Publisher Link]

[7] V.P. Shestopalov et al., "Diffraction gratings (Resonant scattering of waves)," *Kiev: Naukova Dumka*, 1986. [Google Scholar]

[8] Ivan Fedorovych Skitsko, and, Oleksiy Ivanovich Skitsko, "*Physics (Physics for Engineers)*," Igor Sikorsky Kyiv Polytechnic Institute, 2017. [Google Scholar] [Publisher Link]

[9] D.G. Fang, *Antenna Theory and Microstrip Antennas*, 1st ed., CRC Press, 2010. [CrossRef] [Google Scholar] [Publisher Link]

[10] D. Chatterjee, "Paraxial and Source Region Behavior of a Class of Asymptotic and Rigorous (Mom) Solutions in the High-Frequency Planar Limit," *IEEE Antennas and Wireless Propagation Letters*, vol. 4, pp. 71-74, 2005. [CrossRef] [Google Scholar] [Publisher Link]

[11] Yiyang Luo, Vladislav Lusenko, and Sergey Shulga, "Design and Optimization of Sparse Planar Antenna Arrays Based on Special Matrices," *2020 IEEE Ukrainian Microwave Week (UkrMW)*, Kharkiv, Ukraine, pp. 1-6, 2020. [CrossRef] [Google Scholar] [Publisher Link]

[12] L.G. Sodin, "Some Problems of the Theory of Phased Antenna Arrays, Topical for Radio Astronomy," *Radiophysics and Radioastronomy, Radio Astronomy*, vol. 10, no. 5, pp. 128-142, 2005. [Google Scholar] [Publisher Link]

[13] Dmitry Mayboroda, and Sergey Pogarsky, "Microstrip Monopole Antenna with Complicated Topology," *Advances in Information and Communication Technology and Systems: Conference on Mathematical Control Theory*, Kyiv, Ukraine, pp. 394-403, 2019. [CrossRef] [Google Scholar] [Publisher Link]

[14] Guo Qiang et al., "Nonequidistant Two-Dimensional Antenna Arrays Synthesized Using Latin Squares and Cyclic Difference Sets," Radio Physics and Electronics, vol. 24, no. 1, pp. 12-23, 2019. [Publisher Link]

[15] Sergey L. Berdnik et al., "Yagi-Uda Combined Radiating Structures of Centimeter and Millimeter Wave Band," Progress in Electromagnetics Research, vol. 93, pp. 89-97, 2020. [CrossRef] [Google Scholar] [Publisher Link]

[16] V. Khaikin et al., "Instrumental Characteristics of Multibeam Solar Radio Telescope," *3rd ESA Workshop on MM-wave Technology and Applications*, Espoo, Finland, 2003. [Google Scholar]

[17] Alwyn Wootten, and A. Richard Thompson, "The Atacama Large Millimeter/Submillimeter Array," *Proceedings of the IEEE*, vol. 97. no. 8, pp. 1463-1471, 2009. [CrossRef] [Google Scholar] [Publisher Link]